

Using Drag to Hover

Z. Jane Wang

Theoretical and Applied Mechanics,
Cornell University, Ithaca, NY 14853

(Dated: March 20, 2003)

Abstract

Unlike a helicopter, an insect can, in theory, use both lift and drag to stay aloft. Here we show that a dragonfly uses mostly drag to hover by employing asymmetric up and down strokes. Computations of a family of strokes further show that using drag can be as efficient as using lift at the low Reynolds number regime appropriate for insects. Previously, asymmetric strokes employed by dragonflies were viewed as an exception. Here we suggest that these asymmetric strokes are building blocks of the commonly seen symmetric strokes, such as a figure-of-eight or a U-shape. Therefore insects which use those symmetric strokes can also use some drag to hover. In a sense, some insects are rowers or swimmers in air. However unlike oars in water, insects cannot lift their wings out of air. This leads to two subtle consequences. First, a restriction on the degree of asymmetry in the strokes in order to produce sufficient lift. It corresponding to an upper limit in the inclined angle of the stroke plane, about 60° , similar to the value observed in dragonfly flight. Second, a break of symmetry in the forces produced by symmetric strokes.

PACS numbers: 87.19.St, 47.11.+j, 47.32Cc

Airplanes and helicopters are airborne via aerodynamic lift, not drag. However, it is not *a priori* clear that nature should design insects to fly using only lift. In rowing and swimming, we make use of drag to propel, so there is a reason to suspect that insects might do the same.

It is well appreciated that micro-organisms (bacteria, sperm, and protozoa) use drag to swim in low Reynolds number flows[1, 2]. It is also known that some birds and fish use drag to fly and swim in high Reynolds number flows[3, 4]. But recent research on insect flight has primarily focused on the unsteady mechanisms for lift enhancement[5, 6], and seems to have overlooked the useful effects of drag.

The separation of lift and drag, which are force components orthogonal and anti-parallel to the instantaneous velocity of the wing relative to the far field flow, is natural for airplane wings, propeller and windmill blades, and boat sails. This is because large wings and sails ‘fly’ at a relatively steady state and at small angles of attack, so lift is the dominant component. But an insect uses large angles of attack to generate high transient lift, i.e. taking advantage of dynamic stall[7]. At large angles of attack, high lift and high drag go hand in hand, as expected for stalled flow and as seen in recent experiments[8]. Therefore the conventional separation of lift and drag is no longer of central interest. The relevant force for hovering is the net vertical force which balances the gravity; thus it is convenient to decompose the forces into vertical and horizontal components. If a wing is restricted to move *symmetrically* along a horizontal plane, whether in circular helicopter-like or reciprocal motions, the drag roughly cancels in each cycle. And the net vertical force to balance an insect’s weight only comes from lift. In contrast, *asymmetric* up and down strokes along an inclined stroke plane generate vertical forces which are oblique to the stroke plane. The vertical force thus has contributions from both lift and drag.

So at least in theory, drag and lift can be of equal use to insect. But can using drag be as efficient as using lift at the range of Reynolds number appropriate for insects?

Strong evidence suggesting that some insects use drag to hover goes back to an early study by Weis-Fogh[9] who noticed that true hover-flies (Syrphinae) and dragonflies (Odonata) employ asymmetric strokes along an inclined stroke plane. This is in contrast to the symmetric back and forth strokes near a horizontal plane, seen in the majority of hovering insects, including fruit-flies, bees, and beetles. What brought the asymmetric strokes to attention was the failure of quasi-steady calculations in predicting enough vertical forces to support

an insect’s weight[7, 9, 10, 11, 12]. On the other hand, the plunging motion during the down-stroke in the asymmetric strokes certainly indicates that large drag can be generated in the upward direction.

Since the work of Weis-Fogh, the asymmetric strokes have been treated separately from ‘normal hovering’[7, 9]. Most studies have focused on symmetric strokes along a horizontal plane. However, commonly seen insect wing strokes can deviate from the horizontal plane and follow either parabola-like or figure-eight trajectories [13]. Here we suggest that these strokes can be viewed, conceptually, as pairs of asymmetric strokes, illustrated in Fig. 1d and 1e. Because of this connection, we can focus on asymmetric strokes along straight inclined planes, and deduce qualitative results for general symmetric strokes used by insects.

Let us first consider two cases of hovering; one employs symmetric strokes along the horizontal plane, a special case of normal hovering, the other asymmetric strokes along an inclined plane of 60° , suggested by the study of dragonfly free flight(*Aeschna juncea*)[10]. Both cases belong to the family of wing kinematics described by

$$[x(t), y(t)] = \frac{A_0}{2}(1 + \cos 2\pi ft)[\cos \beta, \sin \beta] \quad (1)$$

$$\alpha(t) = \alpha_0 + B \sin(2\pi ft + \phi), \quad (2)$$

where $[(x(t), y(t))]$ is the position of the center of the chord, and β is the inclined angle of the stroke plane (see Fig. 1a-1c). $\alpha(t)$ describes the chord orientation relative to the stroke plane. f is the frequency, A_0 and B are amplitudes of translation and rotation, and ϕ is the phase delay between rotation and translation. α_0 is the mean angle of attack, thus it describes the asymmetry between the up and down strokes. $\alpha_0 = \pi/2$ and $\beta = 0$ correspond to a symmetric stroke along a horizontal plane (Fig. 1c). The wake of this family of wing motions was visualized previously using smoke trajectories[14].

The two dimensional flow around a hovering wing is governed by the Navier-Stokes equation, which is solved here using a fourth order compact finite-difference scheme[15]. To ensure sufficient resolution at the edge of the wing and efficiency in computation, elliptic coordinates fixed to the wing, (μ, θ) , are employed and mapped to a Cartesian grid. The two-dimensional Navier-Stokes equation governing the vorticity in elliptic coordinates is

$$\frac{\partial(S\omega)}{\partial t} + (\sqrt{S}\mathbf{u} \cdot \nabla)\omega = \frac{1}{Re}\Delta^2\omega \quad (3)$$

$$\nabla \cdot (\sqrt{S}\mathbf{u}) = 0, \quad (4)$$

where \mathbf{u} is the velocity field, ω the vorticity field, and S the scaling factor $S(\mu, \theta) = \cosh^2 \mu - \cos^2 \theta$. The forces are calculated by integrating the fluid stress on the wing. Specifically, $\mathbf{F} = \mathbf{F}_p + \mathbf{F}_\nu + \rho W \mathbf{a}$, where \mathbf{F}_p and \mathbf{F}_ν are pressure and viscous contributions, given below, W is the area of ellipse, \mathbf{a} the wing's linear acceleration,

$$\mathbf{F}_p = \rho\nu \int \frac{\partial\omega}{\partial\mu} (\sinh \mu_0 \sin \theta \hat{x} + \cosh \mu_0 \cos \theta \hat{y}) d\theta, \quad (5)$$

$$\mathbf{F}_\nu = \rho\nu \int \omega (-\cosh \mu_0 \sin \theta \hat{x} + \sinh \mu_0 \cos \theta \hat{y}) d\theta. \quad (6)$$

The fictitious forces introduced by the rotating frame, i.e. the centrifugal and Coriolis forces, as well as the force due to rotational acceleration, integrate to zero and thus have no contribution. The method was described in detail previously [12, 16].

The instantaneous forces are nondimensionalized by $0.5\rho u_{rms}^2 c$, where ρ is the density of air, u_{rms} the root mean square of the translational velocity of the center of the wing, and c the chord, respectively. The dimensionless forces are called force coefficients, C_L and C_D denoting the lift and drag coefficients, C_V and C_H are the vertical and horizontal force coefficients. Because the horizontal force cancels over a period, its absolute value is used when taking averages.

The translational motion of the wing is completely specified by two dimensionless parameters, the Reynolds number, $Re \equiv u_{max}c/\nu = \pi f A_0 c/\nu$, and A_0/c . The typical Reynolds number of a dragonfly is about 10^3 , and a fruit-fly is about 10^2 . But since the conclusions drawn below does not crucially depend on the Reynolds number in this range, it is chosen to be 150 for simplicity.

In the case of symmetric stroke (Fig. 1c and Fig. 2a), described by eq. (1) with $\alpha_0 = \pi/2$, and $\beta = 0$, each half-stroke generates almost equal lift in the vertical direction, and almost equal drag in the opposite horizontal direction. The drag in each stroke does not exactly cancel even in the steady state due to a symmetry breaking, as will be discussed. The averaged vertical and horizontal force coefficients are 1.07 and 1.61, respectively, resulting in a ratio of 0.66. In contrast, the asymmetric stroke with $\alpha = 60^\circ$ $\beta = 62.8^\circ$ (Fig. 3a and 3b) generates most of its vertical force during the down-stroke, in which the lift and drag coefficients are 0.45 and 2.4, respectively; they are 0.50 and 0.68 during the upstroke. The

vertical and horizontal force coefficients averaged over one period are 0.98 and 0.75, resulting in a ratio of 1.31, twice the value of the symmetric stroke. In this case 76% of the vertical force is contributed by the aerodynamic drag.

Another view of the difference between the symmetric and asymmetric strokes is revealed by the averaged flow around the wing. The vorticity and velocity fields around the wing at four different times are presented in Fig. 2c and 3c. Comparing the traveling distances of vortex pairs in the two cases suggests a faster jet produced by the asymmetric stroke. A better way to quantify these jets is to plot the time averaged velocity below the wing. The averaged flow shows the structure of the jets, as shown in Fig. 2d and 3d. The velocity is plotted in physical space, which are interpreted from the computed velocity in the body coordinates. The asymmetric stroke generates a faster jet of a width comparable to the chord, and it penetrates downward for about 7 chords. In contrast, the symmetric stroke generates a jet whose width is comparable to the flapping amplitude, and it penetrates down for about 4-5 chords. Thus we tentatively conjecture that dragonflies take advantage of the ground effects to hover above the water at a distance of 7 chords or less, as the jet is reflected by the water.

Next we investigate how the forces and power vary with the degree of asymmetry. For this purpose, it is convenient to fix $A_0/c = 2.5$, $f = 1$, $Re = 150$, $B = \pi/4$, $\phi = 0$, and vary α_0 from $\pi/4$ to $\pi/2$, with ten α 's equally spaced. The time-averaged forces and power are plotted against β , the angle of the stroke plane, in Fig. 4. For a given α_0 , β is determined such that the net force averaged over a period is vertically up. Fig. 4 illustrates two interesting points.

First, as the stroke plane tilts up, the vertical force coefficient, $\overline{C_V}$, remains almost a constant up to $\beta \sim 60^\circ$. The horizontal force averages to zero, but its average magnitude, $\overline{C_H}$ decreases with β . Thus, the ratio, $\overline{C_V}/\overline{C_H}$, increases by a factor of 2 as β increases from 0° to 60° . Therefore by employing asymmetric strokes along an inclined plane, an insect not only maintain the vertical force but also reduces horizontal forces. The averaged power exerted by the wing to the fluid is given by $\overline{P} = \langle F_D(t)u(t) \rangle$, where $F_D(t)$ is the force parallel to the translational velocity of the wing, $u(t)$. Comparing this power with the ideal power based on the actuator disk theory[17] gives a non-dimensional measure,

$$\overline{C_P} = \frac{\langle F_D(t)u(t) \rangle}{\langle F_V(t) \rangle^{3/2}} \sqrt{2\rho A_0}, \quad (7)$$

where the size of the actuator for a two dimensional wing is assumed to be the amplitude A_0 , and F_V is the vertical force. Similar to $\overline{C_V}$, $\overline{C_P}$ is relatively independent of β up to $\beta \sim 60^\circ$. Up to 40° , there is a slight decrease in power required to balance a given weight. Thus using drag to hover does not require extra work.

Second, the sharp decrease in vertical forces at $\beta \sim 60^\circ$ suggests that asymmetric strokes along nearly vertical stroke planes would not generate sufficient force to hover. A quasi-steady model of the forces would not predict such a cut-off[18]. The drop in vertical force is due to the fact that an insect cannot lift its wing out of air, so the wing must interact with its own wake. Such interaction reduces the net vertical force by more than half when $\beta > 70^\circ$. Thus, one might expect that in natural flight the angle of the stroke plane also has an upper limit. Insects using inclined stroke planes appear to fall in this category. One of the largest angles, $\beta \sim 60^\circ$, is observed in dragonflies (*Aeschna juncea*)[10]; other studies reported smaller inclined angles[19].

The interaction between the wing and its wake at these Reynolds numbers has another consequence. Namely, symmetric strokes do not necessarily generate symmetric forces, as would be the case at zero Reynolds number flow. At the Reynolds numbers studied here, the symmetric stroke along the horizontal plane (Fig. 1b) produces a slightly nonzero horizontal force. The symmetry is broken by the initial conditions, whose effects persist in time. Such persistence may seem peculiar at first, but can be explained as follows. The first back and forth stroke generates two pairs of vortices, one at the leading edge and another at the trailing edge. The strengths of these vortex pairs are asymmetric due to the initial motion. Each newly generated vortex is paired with the previous vortex, thus it ‘remembers’ the preceeding stroke. In other words, a sequence of vortices are ‘zipped’ together. Consequently, the vorticity configuration at a given instance can be traced back to the first stroke, thus preserving the initial asymmetry. The nonzero averaged horizontal force, the pwalternating magnitude in the peaks of the lift (Fig. 2b), and the bias in the average flow (Fig. 2c) are manifestations of this asymmetry. Similar broken of asymmetry was observed in a previous theoretical study of butterfly strokes[20]

Real insect wing motions are complex and diverse, and the view of the flapping motion

taken here is simplistic. In addition, the computation is two dimensional, but insects live in three dimensions. Nonetheless, the above analysis provides a new way of thinking about the wing kinematics employed by the insects. In particular, what was perceived as an exception in the biology literature, the asymmetric strokes along an inclined stroke plane, can be viewed as building blocks of more commonly seen symmetric strokes, including the well-known figure-of-eight strokes. Moreover, the upper limit of the stroke plane angle predicted from the computation, 60° , coincides with the maximal angle observed in insects[10]. It also turns out that at least within the family of strokes studied here, using drag is as efficient as using lift. We thus hope that biologists will investigate insect wing kinematics with a new question in mind, that is to what degree insects use drag? Our study further suggests two general lessons. First, to theorists, it seems to be more natural to view insects as swimmers in air rather than small airplanes. Thus instead of refining the unsteady lifting line theory for attached flow, as was appropriate for airplanes, it is more relevant to find a better theory for separated flow. The classical theory of separated flow underpredicts the forces[21]. Second, designing micro-scale flapping mechanisms at very low Reynolds numbers need not follow the traditional rule of optimizing lift, but instead could use both lift and drag.

-
- [1] E. M. Purcell, *Am. J. Phys.* **45**, 3 (1977).
 - [2] G. I. Taylor, *Low Reynolds number flows (video)*, (Encyclopaedia Britannica Educational Corp. (1985).
 - [3] R. W. Blake, *Symp. Zool. Soc. Lond.* **48**, 29 (1981).
 - [4] S. Vogel, *Life in Moving Fluids* (Princeton University, Princeton, N.J., 1996).
 - [5] C. P. Ellington, C. van den Berg, A. P. Willmott, and A. L. R. Thomas, *Nature* **384**, 626 (1996).
 - [6] M. H. Dickinson, F. O. Lehmann, and S. P. Sane, *Science* **284**, 1954 (1999).
 - [7] C. P. Ellington, *Phil. Trans. R. Soc. Lond.* **B 305**, 1 (1984).
 - [8] S. Sane and M. H. Dickinson, *J. Exp. Bio.* **204**, 2607 (2001).
 - [9] T. Weis-Fogh, *J. Exp. Biol* **59**, 169 (1973).
 - [10] R. A. Norberg, In *Swimming and Flying in Nature*(ed. T. Y. Wu, C. J. Brokaw and C. Brennen) **2**, 763 (1975).

- [11] C. Soms and M. W. Luttgers, *Science*, **228**, 1326 (1985).
- [12] Z. J. Wang, *Phys. Rev. Lett.* **85**, 2216 (2000).
- [13] Figure-eight trajectories were reported in early film studies of wing motion^[7]. Recent studies suggested that they are not as common as it was initially assumed (C. P. Ellington, R. Dudley, and M. H Dickinson, private communications). For example, fruit-flies use a plunging motion along a parabolic-like plane (M. H. Dickinson, private communication).
- [14] P. Freymuth, K. Gustafson, and R. Leben, in *Vortex method and vortex motion*, edited by K. Gustafson and J. Sethian (SIAM, Philadelphia, 1991), p. 143.
- [15] W. E and J. Liu, *J. Comp. Phys.* **126**, 122 (1996).
- [16] Z. J. Wang, *J. Fluid Mech.* **410**, 323 (2000).
- [17] J. Leishman, *Principles of Helicopter Aerodynamics* (University of Cambridge, Cambridge, 2000).
- [18] Z. J. Wang (unpublished).
- [19] J. M. Wakeling and C. P. Ellington, *J. Exp. Biol.* **200**, 557 (1997).
- [20] M. Ima and T. Yanagita, *Proceedings of the 50th Japan National Congress on Theoretical and Applied Mechanics* **50**, 237 (2001).
- [21] F. von Karman and J. M. Burgers, in *Aerodynamic Theory*, edited by W. Durand (Springer, Berlin, 1963), pp. vol. 2, Div. E.

Acknowledgement I thank S. Childress, M. Dickinson, C. Ellington, and A. Ruina, P. Lissaman for helpful discussions, and A. Anderson and R. Dudley for suggestions on the manuscripts. The work is supported by AFSOR, NSF, and ONR.

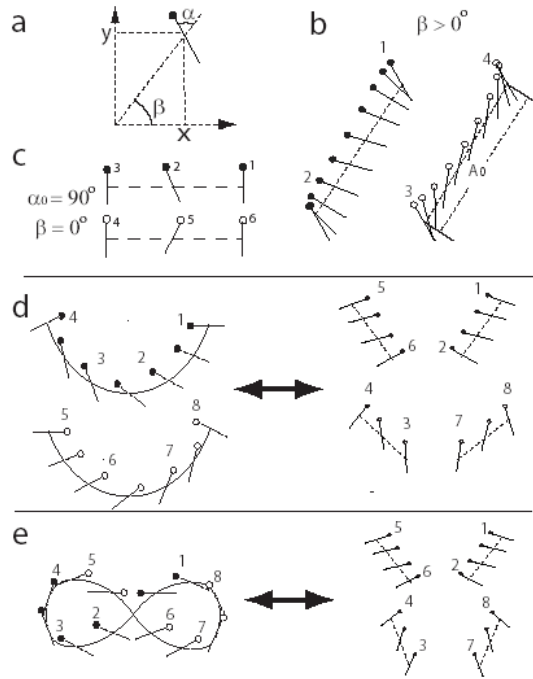


FIG. 1: A family of asymmetric strokes studied in this paper. Solid lines represent chord positions during a stroke. The leading edge is indicated by either a black dot (down-stroke) or an open circle (up-stroke). The numbers next to the leading edges indicate the time sequence. The motion is described by eq. (1) and (2), with A_0 being the end to end amplitude of the stroke, β the inclined angle of the stroke plane (dashed line), and α_0 the initial orientation of the wing. a) definition of the chord position and orientation, b) generic asymmetric strokes c) a special case of symmetric strokes along the horizontal plane. d) symmetric strokes along a parabolic stroke plane, and e) symmetric strokes along a figure-eight. The symmetric strokes in d) and e) can be decomposed into symmetric pairs of the asymmetric strokes described in b). The numbers next to the wings both indicate the time sequence during a stroke, and also identifies the segments on the right hand side in the original stroke. This decomposition allows one to deduce qualitative results for the general symmetric strokes based on the results of asymmetric strokes studied here.

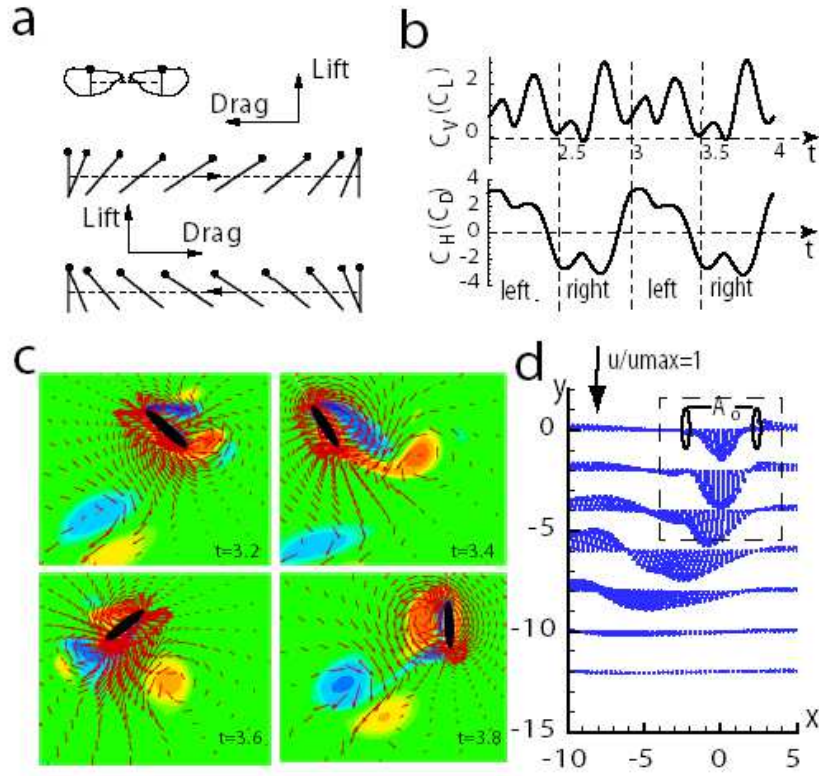


FIG. 2: A special case of normal hovering: symmetric strokes strictly along a horizontal plane. a) wing kinematics given by eq. (1) and (2) with $A_0/c = 2.5$, $\alpha_0 = \pi/2$, $B = \pi/4$, $\beta = 0$. The averaged lift and drag over each stroke are shown in scale. In this case, drag almost cancels in two consecutive strokes, and the vertical force is contributed primarily by aerodynamic lift. b) time dependent vertical (C_V) and horizontal (C_H) force coefficients, which are the same as lift (C_L) and drag (C_D) coefficients. c) snapshots of vorticity (red: counterclockwise rotation, blue: clockwise rotation) and velocity field (red vectors) near the wing, and d) time averaged velocity field over one period, characterized by a downward jet. u_{max} , the maximum translational velocity of the wing is the reference scale. The dashed square corresponds to the region shown in 1c).

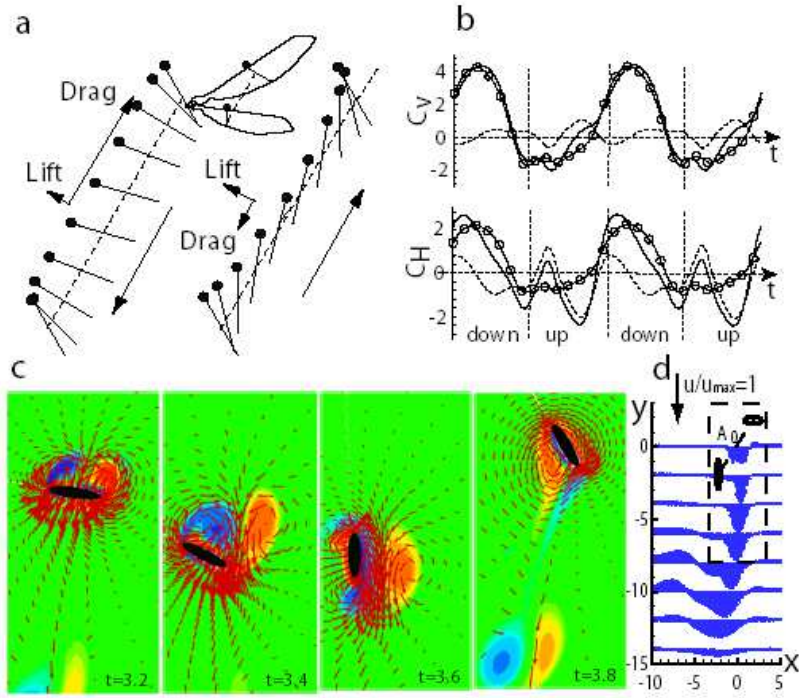


FIG. 3: Hovering along an inclined stroke plane using asymmetric strokes, as seen in dragonfly flight[10]. a) wing kinematics given by eq. (1) and (2) with $A_0/c = 2.5$, $\alpha_0 = \pi/3$, $B = \pi/4$, and $\beta = 0.35\pi$. The averaged lift and drag over each stroke are shown in scale. In this case, the vertical force is contributed primarily by the drag during the down-stroke. b) vertical (C_V) and horizontal (C_H) coefficients (solid lines), and contributions from lift (dashed line), and drag (solid line with circle), c)-d) see the legend of Fig 2.

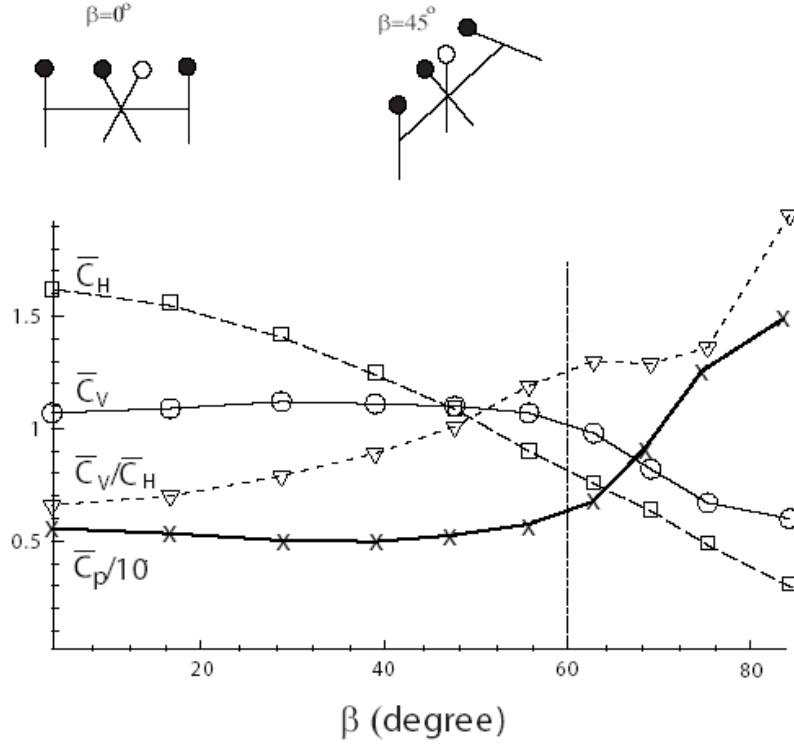


FIG. 4: Comparison of the averaged vertical (\bar{C}_V), horizontal (\bar{C}_H), and power (\bar{C}_P) coefficients as a function of the angle of the stroke plane, β , which characterizes the degree of asymmetry in the up- and down- strokes and the relative contribution of lift and drag to the vertical force. The vertical force remains roughly constant up to $\beta = 60^\circ$, but have a sharp cut-off beyond that, due to the interaction between the wing and its own wake. The magnitude of the horizontal force decreases with β . \bar{C}_P is relatively independent of β up to $\beta \sim 60^\circ$. Up to 40° , there is a slight decrease in power required to balance a given weight. Thus using drag to hover does not require extra work.